RESEARCH PAPER

Effect of titanium content on weld microstructure and mechanical properties of bainitic GMA welds

Jun Seok Seo · Kangmyung Seo · Hee Jin Kim · Changhee Lee

Abstract The effects of titanium content on the weld microstructure, mechanical properties, and inclusion characteristics were investigated in the as-deposited bainitic GMA weld metals having nearly constant level of oxygen content. It was found that titanium addition enhanced the formation of acicular ferrite with the maximum proportion being obtained at ~0.07 wt% Ti. The resultant change in weld microstructure with titanium content was well reflected in the Charpy impact toughness showing the lowest ductile-brittle transition temperature at 0.07 wt% Ti. Detailed TEM and STEM analysis preformed on weld metal inclusions demonstrated that the maximum acicular ferrite recorded in this weld is mainly attributable to the formation of manganese-depleted zone (MDZ) associating with the formation of nonmetallic inclusions dominant with Ti_2O_3 phase.

Keywords GMA welding · Weld metal · Microstructure · Titanium · Inclusions

J. S. Seo
Technical Research Center, Hyundai Steel Co., 167-32, Kodaeri Songakeup, Dangjinsi 343-823, Republic of Korea

K. Seo · C. Lee
Division of Materials Science and Engineering, Hanyang University, 17 Haengdang-dong, Seongdong-gu, Seoul 133-791, Republic of Korea

H. J. Kim (✉)
Korea Institute of Industrial Technology, 35-3 Hongchonri, Ibjangmyun, Chonansi 330-825, Republic of Korea
e-mail: kimhj@kitech.re.kr

1 Introduction

It has been well established that weld metal mechanical properties are strongly dependent on weld microstructure, especially on the proportion of acicular ferrite microstructure. Due to the fine nature of this microstructure, it can improve the weld metal strength and toughness simultaneously [1]. Accordingly, numerous investigators have studied the various factors such as: (i) chemical composition of welds, (ii) cooling rate in the temperature range of 800–500 °C, (iii) size of prior-austenite grains, and (iv) inclusion characteristics to investigate their effect on the formation of acicular ferrite. Regarding those factors, comprehensive reviews [1–4] were also made frequently.

When the considering factors are limited to the chemical composition, titanium would be the one that is unique for the formation of weld metal microstructure. Following the pioneer work by Ito and Nakanishi [5] in 1976, systematic studies on the effect of titanium content were accomplished by Evans in the various ferritic welds [6–9] and also in the bainitic weld [10]. According to his results, acicular ferrite content increases dramatically with a small amount of titanium addition and reaches its maximum of ~70 % at ~30 ppm titanium. Interestingly, a slightly lower but still high level of ferrite content over ~60 % was reported to be obtained in a wide range titanium concentration from 250 to 580 ppm without showing any noticeable second peak.

As, in Evans' studies, no sharp second peak was recorded over such a wide range of titanium content, it would be worth to figure out the variation of acicular ferrite content in the even higher region of titanium concentration over 600 ppm. Another fact noted in the Evans' results is that the oxygen content of welds varies significantly with titanium content. As the oxygen content has been known to play an important role in determining the acicular ferrite content [5, 11, 12], the variations of acicular ferrite content reported by Evans might not be

the true effect of titanium content alone but a combined effect of titanium and oxygen. In order to overcome these limitations, present authors [13] have investigated two gas metal arc (GMA) bainitic welds that contained similar oxygen content but had different titanium concentration of 0.002 and 0.072 wt%, and found a significant increase in acicular ferrite content to over 90 % in the high titanium weld. This result stimulates further work on weld microstructures that can be developed in range between those two concentrations as well as over 0.072 wt%. Thus, the goal of the present study is to examine the pure titanium effect over a wider range of titanium content and, if possible, to suggest the optimum titanium concentration that allows maximum acicular ferrite content in the bainitic GMA weld.

2 Experimental procedures

2.1 Preparation of experimental welds

The welds investigated in this study were all prepared with bead-in-groove GMA welding. As described in the previous report [13] and shown in Fig. 1, a two-step welding was performed with AWS ER100S grade wire and Ar+20 % CO_2 shielding gas. Table 1 gives the chemical compositions of the base plate and welding wire employed in this investigation. Using these materials, buttering welds were deposited to fill the 10 mm deep groove. A total of five buttering plates were prepared and each of them was used for the subsequent experimental welds. Prior to experimental bead-in-groove welding, 5 mm deep V-groove was made at the center of the buttering weld and then pure titanium fibers of 0.3 mm in diameter were inserted in the slot that was made at the bottom of the groove. The number of fibers inserted was zero to four so that a total of five experimental welds could be made by subsequent single-pass bead-in-groove welding, all different in titanium content. All the microstructural and inclusions analyses were performed at the center of the experimental welds as marked by circle in

Fig. 2a. Oxygen content was determined at the same location as that of microstructural analysis by inert gas fusion method and other elements were analyzed by an optical emission spectrometer (OES).

### 2.2 Metallographic examination and inclusion analysis

Optical microscope (OM) examinations were carried out on transverse sections of weld metals etched with 2 % Nital solution. From the optical micrographs taken at ×500 magnification, the proportion of acicular ferrite was measured by a point-counting method. Inclusion size distribution and density were determined using backscattered SEM images taken at a magnification of ×10,000 from polished and unetched OM specimens. To obtain reliable data, a minimum of 300 particles was counted in each weld. In addition, inclusions were extracted by an electrolysis technique [14], and their overall chemistry was examined by energy dispersive X-ray spectrometer (EDX) in SEM.

For the selected samples, inclusion phases were investigated by analytical transmission electron microscope (ATEM) in TEM and STEM mode. Thin foil specimens were prepared by twin-jet polishing followed by several steps of ion milling. Twin-jet polishing was performed in a solution of 5 % perchloric acid+95 % methanol and at 228 K. In order to visualize the distribution of each phase, the elemental mapping was also carried out using EDX in STEM mode. Quantitative EDX line scanning was also performed across the inclusion/matrix interface to reassess our previous result [13] showing the manganese depletion in adjacent matrix qualitatively.

2.3 Mechanical tests

Vickers hardness was measured using a 98-N (10 kg) load. Five measurements were made on each specimen and the average values were plotted as a function of titanium content. In addition, subsize (10×5 mm) Charpy V-notch specimens were machined with a notch located at the center of the

Fig. 1 Preparation of experimental welds to have different titanium content
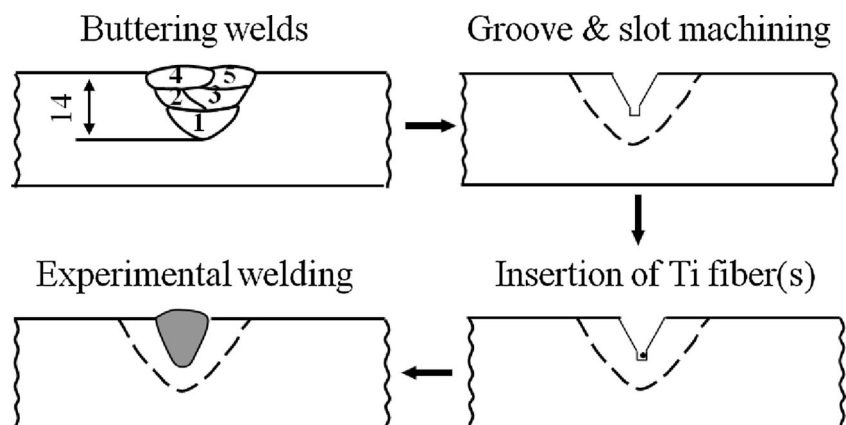
Table 1 Chemical compositions (wt%) of the base metal and welding wire used

Material	C	Si	Mn	P	S	Cr	Ni	Mo	Al	Ti
Base metal	0.04	0.25	1.56	0.008	0.004	0.30	0.23	0.06	0.04	0.018
Welding wire	0.06	0.32	1.53	0.006	0.007	0.26	1.93	0.34	0.01	0.005

experimental weld metal Fig. 2b. Impact tests were performed at various temperatures down to −120 °C to construct full ductile-to-brittle transition curves.

3 Result and discussion

3.1 Weld metal chemical composition

The chemical compositions of all experimental welds labeled as 0Ti, 1Ti, 2Ti, 3Ti, and 4Ti are given in Table 2. Numbers in each ID are the number of fibers inserted in the groove before depositing the experimental welds. As shown in Table 2, the chemical compositions of all welds were remarkably consistent with the exception of titanium. The weld made without fiber addition (0Ti) recorded a titanium concentration of 0.002 wt% that is somewhat lower than that of welding wire (0.005 wt%). With titanium fibers, the titanium concentration of weld metals increases linearly with the number of fibers and reaches to 0.091 wt% in the 4Ti weld. Such a wide variation in titanium content, however, little affects the concentrations of other oxidizing elements; silicon being varied from 0.20 to 0.23 wt%, manganese from 1.28 to 1.31 wt.%, and aluminum from 0.005 to 0.006 wt%.

Of important note in Table 2 is the oxygen content of the five welds, all falling within a narrow range of 330∼366 ppm. This result is contrary to the trend that was reported in the shielded metal arc welding (SMAW) welds in which the oxygen content decreased from 449 to 292 ppm with increasing titanium content of weld metals from 0 to 580 ppm [9]. This discrepancy in

oxygen content with titanium may result from the difference in welding processes and also in the method of adding titanium; SMAW welds being made by titanium powders to the electrode coatings vs. gas metal arc welding (GMAW) welds by insertion of titanium fibers within the groove. Whatever the reasons are, the constant oxygen content of the present welds allowed us to investigate the pure effect of titanium on weld microstructure at the same level of oxygen content.

3.2 Weld microstructure

Optical micrographs taken from the center of the experimental welds are shown in Fig. 3. Due to a bainitic composition of the present welds, the formation of primary ferrite (PF(G)) along austenite grain boundaries was inhibited in all of the present welds. Instead, what appeared in the weld microstructures is a mixture of acicular ferrite (AF) and bainite, their proportions being varied appreciably with the titanium concentration. A mixed microstructure of acicular ferrite and bainite forms in the low titanium welds like 0Ti and 1Ti while a microstructure fully packed with acicular ferrite was developed in 2Ti and 3Ti welds. A further increase in titanium content to that of 4Ti weld (0.09 wt%) results in a mixed microstructure again.

The proportions of acicular ferrite measured from each weld are plotted in Fig. 4 as a function of titanium content. These results reveal that a minimal amount of titanium, of the order of 0.002 wt%, can produce ∼50 % acicular ferrite but an addition to ∼0.02 wt% leads to a slight decrease in acicular ferrite content, indicating that titanium addition is not always beneficial for acicular ferrite formation. Further addition of

Fig. 2 Macro section of welded specimen showing (**a**) the bead contour of experimental weld along with the location of microstructural analysis and (**b**) the notch location of Charpy impact test specimen
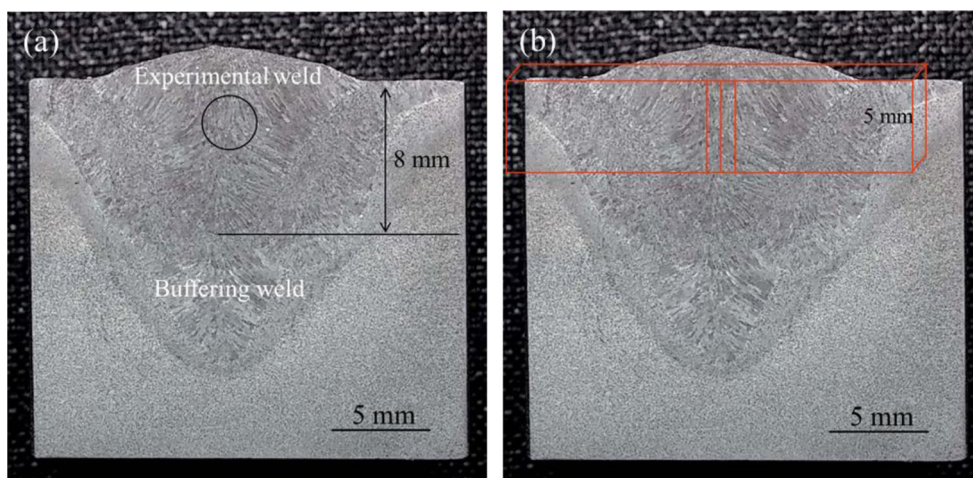
Table 2 Chemical compositions of the weld metals in wt% except oxygen and nitrogen (ppm)

ID	C	Si	Mn	Al	Ni	S	Ti	O	N
0 Ti	0.07	0.20	1.31	0.005	1.80	0.006	0.002	347	126
1 Ti	0.06	0.20	1.31	0.006	1.82	0.006	0.023	351	115
2 Ti	0.06	0.21	1.29	0.006	1.83	0.006	0.049	330	113
3 Ti	0.06	0.22	1.28	0.006	1.80	0.006	0.072	366	118
4 Ti	0.06	0.23	1.28	0.006	1.82	0.006	0.091	353	114

Others: 0.24Cr-0.34Mo-0.20Cu

titanium shows a profound effect on acicular ferrite formation showing a maximum of 92 % at ~0.07 wt% (3Ti weld). Referring to the previous results reported for Ti-free welds being very low in acicular ferrite content but for 30~40 ppm titanium welds being encountered maximum ferrite content [6, 7], the expected trend can be drawn further down to 0 wt% as shown with a dotted line in Fig. 4. Such an extension illustrates that the possible presence of the first peak near 30 ppm titanium might be missed in the present study.

3.3 Inclusion size and density

Figure 5 shows the effect of titanium content on the geometric factors of inclusions, i.e., the inclusion size denoted as the average diameter and the number density of inclusions. As can be expected from the fact that all the present welds are similar in oxygen content, both factors are nearly constant and little affected by titanium content, inclusion sizes being in the range of 0.40~0.46 μm and their densities in $(13~15)\times10^3/mm^2$. From this result, it could be concluded that little correlation exists between acicular ferrite content and geometric factors of inclusions. This fact is important to be noted because it allows us to take out the geometric factors in interpreting the variation of acicular ferrite content shown in Fig. 4. Hence, the acicular ferrite content of the present welds is thought to be related to a change in chemical and crystallographic feature of inclusions when the weld metal hardness is not largely different.

3.4 Mechanical properties

Figures 6 and 7 show the effect of titanium content on weld metal hardness and toughness, respectively. It can be seen that titanium content led to little change in hardness but greatly affected the toughness. As shown in Fig. 6, all the hardness data fall in a narrow range of 265~270 Hv suggesting that the resultant variation in toughness is mostly attributable to the microstructural change shown in Figs. 3 and 4. Figure 7a shows the ductile-brittle transition curves shifting significantly depending on the titanium content. Both 2Ti and 3Ti record the lowest ductile-brittle transition temperature (DBTT) of

~80ºC along with high upper-shelf energy while 0Ti and 1Ti welds exhibit the highest DBTT with very low upper-shelf energy.

As the present welds are quite similar not only in hardness but also in geometric factors, the toughness variation shown in Fig. 7a could be explained as a result of microstructural variation, especially in acicular ferrite content. In addition, the impact toughness at −60ºC plotted in Fig. 7b as a function of titanium content shows a trend that is very similar to that of acicular ferrite content shown in Fig. 4. This fact further suggests that there is a strong correlation between weld metal toughness and the acicular ferrite content of the welds.

Previously, Johnson and others [10] studied the influence of titanium additions on mechanical properties of bainitic SMA welds and their results shows that first peak in impact toughness appears at ~40 ppm titanium and second plateau is in over 250 ppm. As the present 0Ti weld contains about 20 ppm titanium, it would not be enough to get high impact toughness like the first peak toughness encountered by Johnson et al. [10].

3.5 Inclusion chemistry

From each weld, several extracted particles over 1 μm in size were selected for EDX spot analysis in SEM and the average compositions are shown in Table 3. In this table, oxygen is deliberately omitted owing to the severe convolution with titanium L and manganese L peaks and thus the mean atomic percent ratios of metallic elements are listed for each weld. In the 0Ti weld (0.002 wt% Ti), manganese and silicon are the main metallic elements in the inclusion, indicating manganese silicate is a major phase of the inclusions in this weld. With increasing titanium content of the welds, an overall increase in titanium content within the inclusions is observed. In 3Ti and 4Ti welds, titanium becomes the predominant element of the inclusion and no silicon is involved in the inclusion formation implying that silicon is more sensitive to the addition of titanium than manganese. In contrast, aluminum is shown to be insensitive to titanium addition, which is possibly because aluminum oxidizes prior to the titanium reaction.

3.6 Inclusion phases and MDZ analysis

In the present investigation, 0Ti and 3Ti welds are chosen for ATEM analysis focusing on the constituent phases formed in inclusions and on the presence of manganese-depleted zone (MDZ) in the surrounding matrix. Although a large number of inclusions were characterized for each weld, the following summaries typical results obtained.
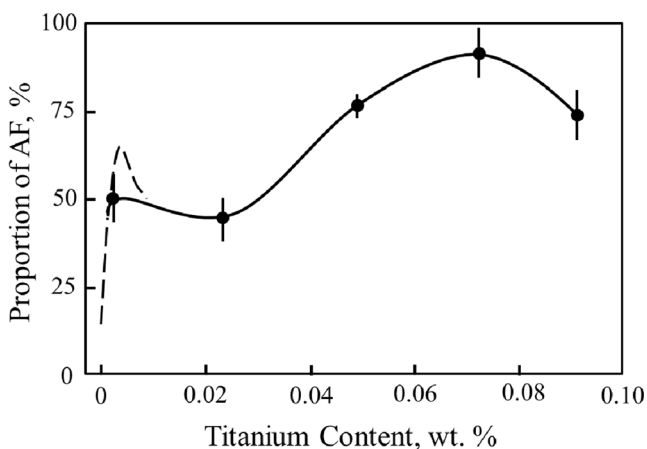
3.6.1 0Ti Weld (0.002 wt% Ti)

The elemental EDX mapping obtained from a typical inclusion in 0Ti weld are given in Fig. 8. As reported

Fig. 3 Optical micrographs of
weld metals: **a** 0Ti, **b** 1Ti, **c** 2Ti **d**
3Ti and **e** 4Ti weld
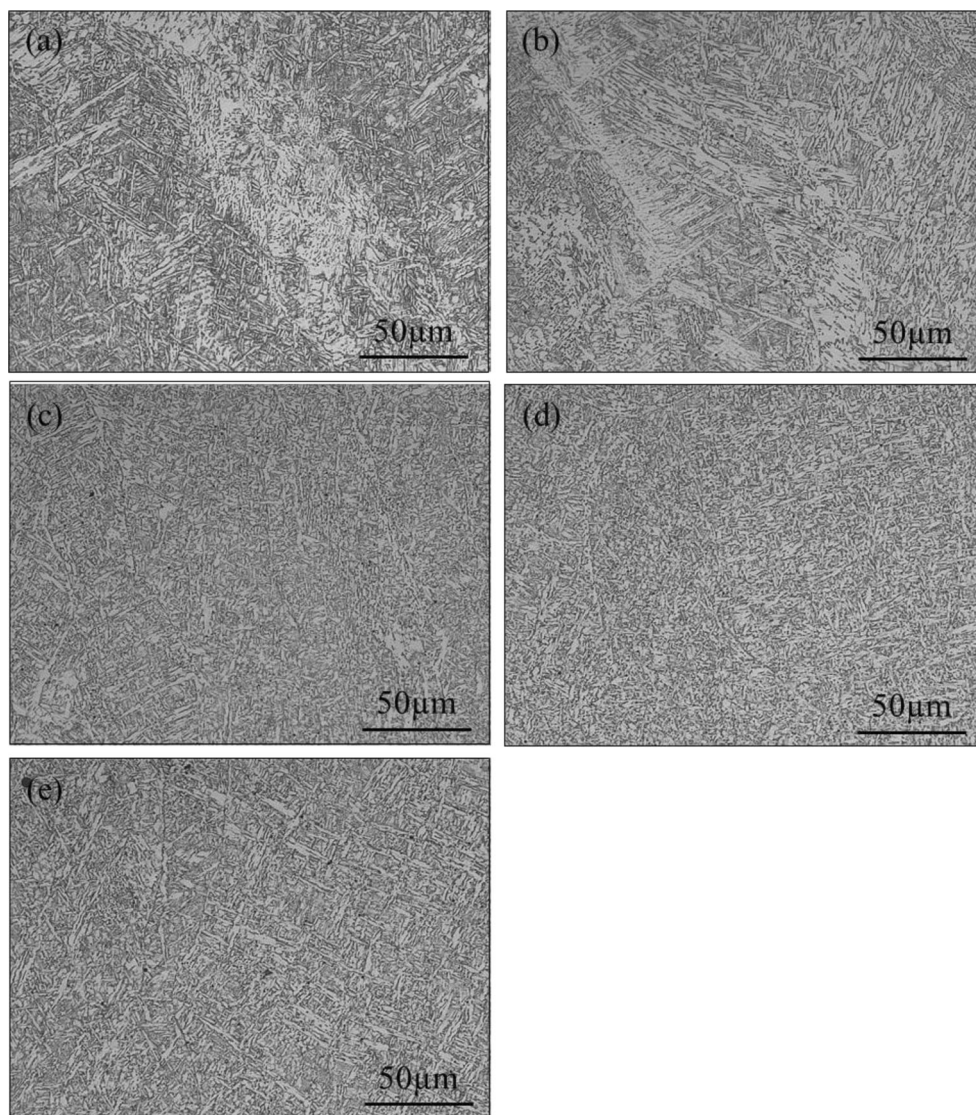
previously [13], the bulk phase is amorphous (Mn, Al)-silicate having a uniform distribution of elements and this

**Fig. 4** Proportion of acicular ferrite as a function of titanium content

phase is often partly covered with MnS and titanium-rich oxide layers. Titanium-rich phase has been confirmed to be a certain type of (Mn, Ti)-oxide as it turned out to be rich in manganese as well. EDX line scanning was performed across the titanium-rich layer as shown by arrow in STEM image of Fig. 8, and the concentration profiles of manganese and titanium in wt% are shown in Fig. 9. From this result, it is clear that there is no noticeable drop in manganese concentration in the matrix near inclusion surface and thus no MDZ formation in this weld. Therefore, even though it is not clear how the titanium-rich phase can be formed on the surface of manganese silicate glass, it is believed that (Mn, Ti)-oxide layer plays a certain role on acicular ferrite nucleation and thus on the formation of an appreciable fraction of acicular ferrite, nearly 50 % (Fig. 4). However, it still remains to examine how this surface phase promotes the nucleation of acicular ferrite to some extent.

(a)

(b)
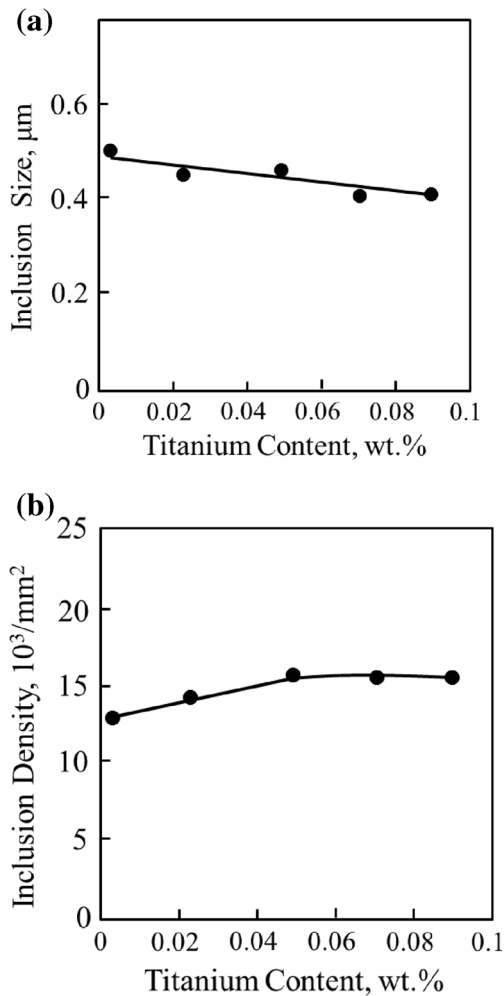
Fig. 5 Variations of **a** inclusion size and **b** density with titanium content

3.6.2 3Ti Weld (0.072 wt% Ti)

This weld is the one that recorded the maximum in acicular ferrite content (Fig. 4), implying that the inclusions in this weld are very high in nucleation potency for acicular ferrite nucleation. EDX elemental maps for a typical inclusion are
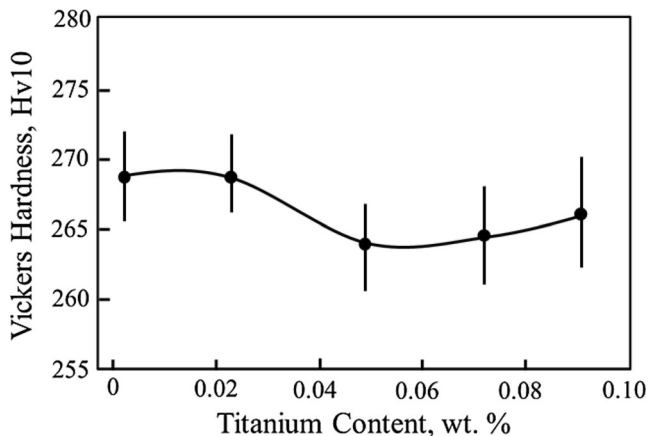
Fig. 6 Hardness variation with titanium content

(a)

(b)
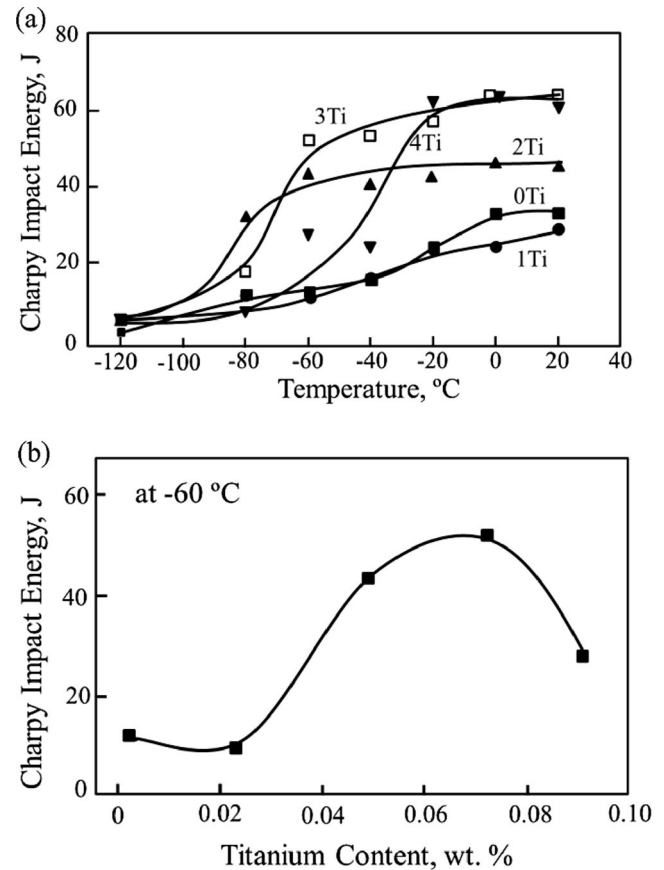
Fig. 7 Results of Charpy impact tests showing the effect of titanium on weld metal toughness: (**a**) ductile-brittle transition curves, (**b**) Charpy impact energy at −60ºC

shown in Fig. 10. These maps illustrate that the inclusion comprises two distinct phases, i.e., Ti-rich phase as a major constituent and Al-rich phase as a minor. It can be seen in the manganese map that Ti-rich phase further divides into two regions due to the difference in manganese content. In the previous investigation [13], Al-rich phase was identified as γ-Al_2O_3 and Ti-rich phases were all identified as Ti_2O_3 regardless of manganese content.

Nitride has been often expected to be formed on the inclusion surface [15, 16] but careful light element EDX analyses failed to detect nitrogen in any regions of the inclusions studied and so it was concluded that all titanium is present as oxides and nitride phase like TiN has not been formed

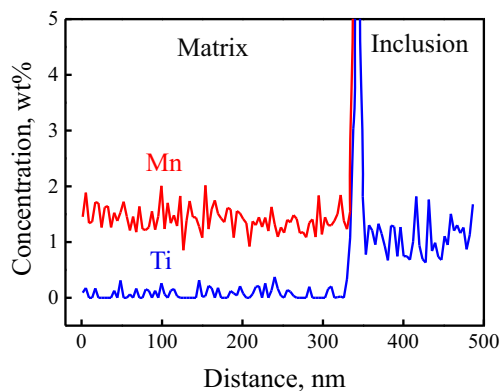**Table 3** Result of EDX spot analysis on extracted inclusion particles (at% ratio)

ID	Ti	Mn	Al	Si
0 Ti	2	46	12	40
1 Ti	26	42	13	19
2 Ti	62	17	17	3
3 Ti	74	14	11	0
4 Ti	78	7	15	0

Fig. 8 STEM-EDX elemental mapping images of a typical inclusion formed in 0Ti weld, showing the titanium-rich layer developed on the inclusion surface
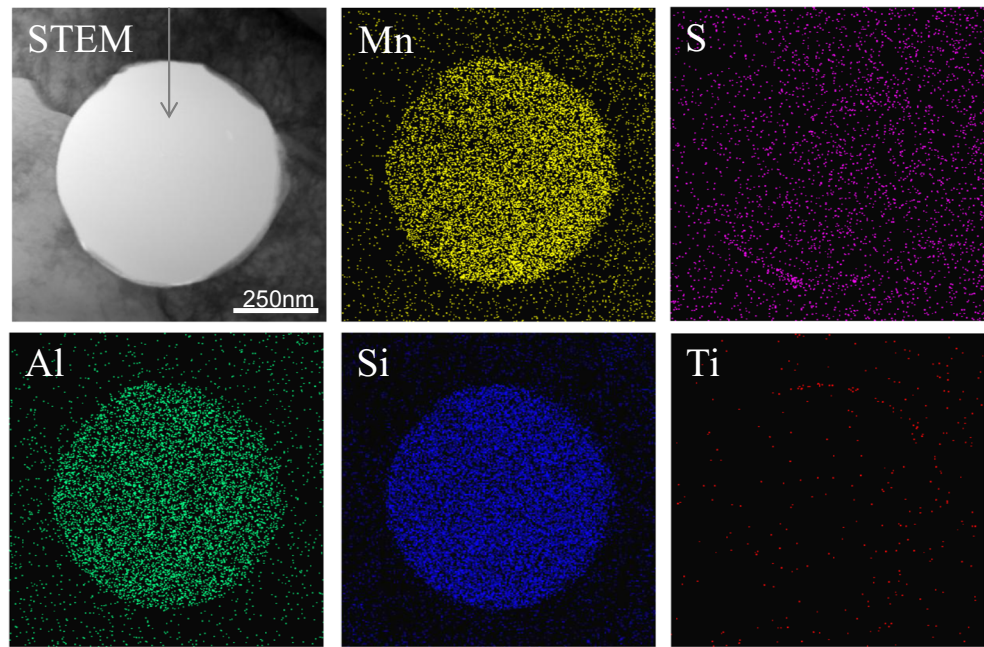
associating with oxide inclusions in this weld even though it contains high titanium and nitrogen contents (Table 2).

From the manganese image in Fig. 10, it is apparent that this inclusion is surrounded by dark band, indicating that manganese-depleted zone (MDZ) may exist around this inclusion. As the previous investigation also demonstrated the development of MDZ in the surrounding matrix, attempts were made in this study to measure the manganese concentration across the interface region by EDX line scanning. / Fig. 11 show the concentration profile of manganese along the line drawn in bright field TEM image and that of nickel measured as for the reference. In contrast to nickel, the manganese concentration is lower in the regions close to the inclusion than in the bulk. This result indeed shows the presence of MDZs in both sides of inclusion, and the minimum concentration of manganese in MDZ is about 0.5 wt% compared to 1.3 wt% in the bulk matrix. Such an EDX

analysis was performed on three more inclusions and the extent of Mn depletion (ΔMn) in MDZ was calculated with following equation:

$$\Delta Mn = \text{average Mn content in matrix} - \text{minimum Mn content in MDZ}$$

As shown in Table 4, the Mn depletion calculated is in the range of 0.5~0.8 at.%. Referring to the theoretical calculation

Fig. 9 Result of EDX line scanning across the titanium-rich layer along the arrow mark shown in STEM image of Fig. 8
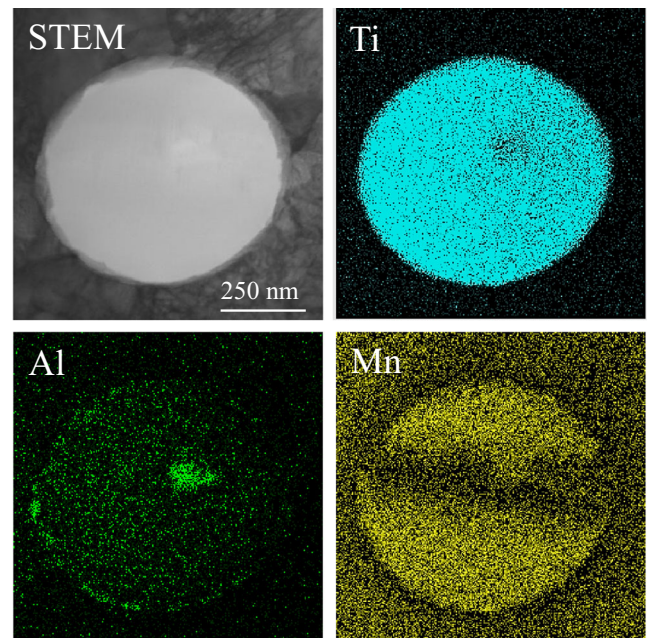
Fig. 10 STEM and EDX elemental mapping images of an inclusion formed in 3Ti weld, showing a titanium oxide inclusion surrounded by a dark band in manganese mapping image

Fig. 11 Concentration profiles of manganese and nickel along the red line drawn in bright field (BF) image of inclusion shown in Fig. 10
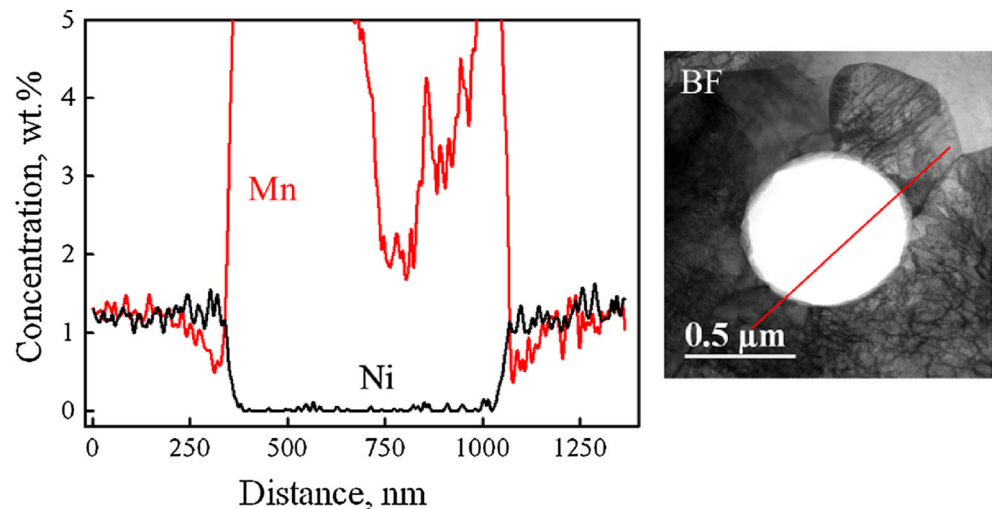
on austenite to ferrite transformation temperature being dropped about 35 °C per wt% Mn [17], the local increase in the transformation temperature of present MDZs can be estimated to be about 18∼28 °C. Even though the consideration of bainite nucleation from grain boundaries is beyond the scope of the present study, MDZ formation can increase the chemical driving force for $\gamma \rightarrow \alpha$ transformation and thus make Ti_2O_3 inclusions more effective for acicular ferrite formation, resulting in the maximum proportion of acicular ferrite in 3Ti weld.

Over the years, several suggestions have been put forward to explain why acicular ferrite nucleates on inclusions [18]. Good lattice matching between inclusion and ferrite appears to be a popular explanation for the nucleation from titanium-containing inclusions and was supported by the experimental evidences obtained for the TiO phase [19]. However, hexagonal Ti_2O_3 shall be expected to offer poor lattice matching with bcc ferrite. Another mechanism possible for titanium-containing phase is the MDZ formation and its formation have been well demonstrated in the titanium-killed steels associating with Ti_2O_3 inclusions [20, 21], but very little evidence has been established for the weld metals. The present result, however, gives clear evidences that MDZ can be developed in weld deposits when the titanium content is high enough to form Ti_2O_3 inclusions. These findings, however, do not rule out the possibility of other mechanisms because there are

increasing evidences that the degree of lattice misfit with α-iron is important in the nucleation of acicular ferrite especially when the TiO phase forms on the inclusion surface [19].

4 Conclusions

Systematic studies were carried out to investigate the effect of titanium content on weld microstructure, mechanical properties, and inclusion characteristics in the bainitic-type GMA welds having similar oxygen content. Based on the results, the following conclusions can be drawn;

(1) As-deposit microstructure of bainitic GMAW welds consists of bainite and acicular ferrite, their proportions being varied with titanium content in weld metal. A trace of titanium of the order of 20 ppm can produce a weld microstructure with ∼50 % acicular ferrite while an addition of titanium to ∼0.02 wt% slightly decreases the acicular ferrite content. A further increase in titanium promotes the formation of acicular ferrite reaching its maximum of over 90 % at ∼0.07 wt% Ti.

(2) The variation in impact toughness could be well explained following the microstructural change with titanium content, i.e., the higher the acicular ferrite is the better the weld metal toughness.

Table 4 The extent of Mn depletion measured in EDX line scanning

Inclusion #	Ave. Mn in matrix (at%)	Min. Mn in MDZ (at%)	Mn depletion (at%)
#1	1.30	0.50	0.79
#2	1.33	0.57	0.77
#3	1.21	0.50	0.71
#4	1.28	0.80	0.48

(3) Inclusion chemistry changes greatly with titanium content of weld metal. At titanium concentration of ~0.07 wt%, inclusions dominant with Ti_2O_3 are formed and these inclusions are surrounded with MDZ. Therefore, the maximum ferrite content observed ~0.07 wt% Ti can be explained by the formation of MDZ associating with Ti_2O_3 inclusions.

References

1. Sarma DS, Karasev AV, Jonsson PG (2009) On the role of non-metallic inclusions in the nucleation of acicular ferrite in steels. ISIJ Int 49(7):1063–1074

2. Abson DJ, Pargeter RJ (1986) Factors influencing as-deposited strength, microstructure, and toughness of manual metal arc welds suitable for C-Mn steel fabrications. Int Met Rev 31(4):141–193

3. Ohkida S, Horii Y (1995) Recent development in controlling the microstructure and properties of low alloy steel weld metals. ISIJ Int 35(10):1170–1182

4. Koseki T, Thewlis G (2005) Inclusion assisted microstructure control in C-Mn and low alloy steel welds. Mater Sci Technol 21(8):867–879

5. Ito Y, Nakanishi M (1976) Study on Charpy impact properties of weld metal with submerged arc welding. Sumitomo Search 15:42–61

6. Evans GM (1992) The effect of titanium in SMA C-Mn steel multipass deposits. Weld J 71(12):447s–454s

7. Evans GM (1993) The effect of titanium in manganese-containing SMA weld deposits. Weld J 72(3):123s–133s

8. Evans GM (1995) Microstructure and properties of ferritic steel welds containing Al and Ti. Weld J 74(8):249s–261s

9. Evans GM (1996) Microstructure and properties of ferritic steel welds containing Ti and B. Weld J 75(8):251s–260s

10. Johnson MQ, Evans GM, Edwards GR (1995) The influence of titanium additions and interpass temperature on the microstructures and mechanical properties of high strength SMA weld metals. ISIJ Int 36(10):1222–1231

11. Onsoien MI, Liu S, Olson DL (1996) Shielding gas oxygen equivalent in weld metal microstructure optimization. Weld J 75(7):216–224

12. Seo JS, Lee C, Kim HJ (2013) Influence of oxygen content on microstructure and inclusion characteristics of bainitic weld metals. ISIJ Int 53(2):279–285

13. Seo JS, Kim HJ, Lee C (2013) Effect of Ti addition on weld microstructure and inclusion characteristics of bainitic GMA welds. ISIJ Int 53(5):880–886

14. Park SH, Hong KJ, Jung SO, Shin KS (2001) Phase analysis of precipitates and inclusions in steels. Trends Metal Mater Eng 14(4):2–7 (in Korean)

15. Es-Souni M, Beaven PA (1990) Microanalysis of inclusion/matrix interfaces in weld metals. Surf Interface Anal 16:504–509

16. Kluken AO, Grong O (1989) Mechanisms of inclusion formation in Al-Ti-Si-Mn deoxidized steel weld metals. Metall Trans A 20A(8):1335–1349

17. Kang Y-B, Lee H-G (2010) Thermodynamic analysis of Mn-depleted zone near Ti oxide inclusions for intragranular nucleation of ferrite in steel. ISIJ Int 50(4):501–508

18. Babu SS (2004) The mechanism of acicular ferrite in weld deposits. Curr Opinion Solid State Mater Sci 8:267–278

19. Yamada T, Terasaki H, Komizo Y (2009) Relation between inclusion surface and acicular ferrite in low carbon low alloy steel weld. ISIJ Int 49(7):1059–1062

20. Byun J-S, Cho YW, Chung SH, Shim J-D, Lee DN (1999) Nucleation of intragranular ferrite at Ti_2O_3 particle in low carbon steel. Acta Materialia 47(9):2751–2760

21. Byun J-S, Shim J-H, Cho YW, Lee DN (2003) Non-metallic inclusion and intragranular nucleation of ferrite. Acta Meterialia 51:1593–1606